

Chemotaxis-Induced Anomalous Tracer Diffusion in Bacterial Suspensions

Zihan Huang, Pengyu Chen, Guolong Zhu, Yufei Cao, and Li-Tang Yan*
*Key Laboratory of Advanced Materials (MOE), Department of Chemical Engineering,
 Tsinghua University, Beijing 100084, P. R. China*

(Dated: December 3, 2024)

Chemotaxis, a basic and universal phenomenon among living organisms, directly controls the transport kinetics of active fluids such as swarming bacteria, but has not been considered when utilizing passive tracer to probe the nonequilibrium properties of such fluids. Here we present the first theoretical investigation of the diffusion dynamics of a chemoattractant-coated tracer in bacterial suspension, by developing a molecular dynamics model of bacterial chemotaxis. We demonstrate that the non-Gaussian statistics of full-coated tracer arises from the noises exerted by bacteria, which is athermal and exponentially correlated. Moreover, half-coated (Janus) tracer performs a composite random walk combining power-law-tail distributed Lévy flights with Brownian jiggling at low coating concentration, but undergoes an enhanced directional transport when coating concentration is high. Particularly, such transition is identified to be second-order, with a critical exponent 1.5 independent of bacterial density. Our findings reveal the fundamental nonequilibrium physics of active matter under external stimuli, and underscore the crucial role of asymmetrical environment in regulating the transport processes in biological systems.

Active responses to external stimuli in living systems, which help organisms to realize adaptive behaviors in changing environments, ubiquitously affect the inner working and collective motion of complex biological fluids. Like the magnetoreception in bird migration for acclimatization to climate [1], and Lévy walks in animal movements for optimal foraging [2], the transport kinetics of such active fluids with stimulus responses allows a pivotal approach to reveal the fundamental statistical physics of nonequilibrium systems. In particular, chemotaxis [3], the biased movement of motile organisms towards or away from chemical stimuli, offers a direct means to control the collective dynamics of active systems [4, 5] and to realize simple yet effective searching strategy for targets with chemotactic signal [6]. Therefore, the chemotactic process has been widely investigated for centuries, especially bacterial chemotaxis [7–12]. As the simplest organism performing chemotactic behaviors, bacteria are highly accessible and relatively easy to trace, thereby making them a paradigm to understand the mechanism of chemotaxis [7–10] and to be harnessed for drug delivery [13], sensing [14] and mobile devices [15].

On the other hand, as a system with net incoming flux of energy, the suspensions of motile bacteria demonstrate a rich variety of intriguing nonequilibrium phenomena such as targeted delivery [16], ratchet motors [17, 18] and violation of fluctuation-dissipation theorem [19]. Thus, exploring the exotic features and potential applications of such active media is of great physical and biological importance. A reliable and universal method to probe their inherent properties is analyzing the diffusion dynamics of a passive tracer immersed in bacterial bath [19–25]. Rather than in the conventional equilibrium media, anomalous behaviors of tracer including enhanced transport [20] and non-Gaussian statistics [21] are widely observed, as a consequence of the intrinsic peculiarities

of bacterial suspensions. However, chemotaxis, which is a basic and universal phenomenon among motile bacteria and directly controls the motion of bacterial cells, has not been addressed in those previous works. Thus, the unrevealed nonequilibrium physics of swarming bacteria under chemotactic stimuli makes it an urgent and striking issue to explore the tracer diffusion in bacterial bath coupled with chemotaxis.

In this Letter, we report the first theoretical study of tracer statistics in bacterial suspensions where chemotactic responses are considered. The model of bacterial chemotaxis is developed based on run-and-tumble dynamics and Monod-Wyman-Changeux (MWC) model, to study the diffusion dynamics of an isolated chemoattractant-coated spherical tracer in bacterial suspension. For full-coated tracer, we demonstrate that bacterial noise, i.e., collisional forces exerted by bacteria, which is athermal and exponentially correlated, directly leads to the non-Gaussian statistics of tracer. Moreover, when increasing the coating concentration, half-coated (Janus) tracer undergoes a second-order phase transition from a composite random walk to an enhanced directional transport, with a critical exponent 1.5 independent of bacterial density. Our findings allow a significant advance in revealing the fundamental nonequilibrium physics of active matter under external stimuli.

The motion of bacteria is modeled based on the run-and-tumble dynamics of *E. coli* [26]. As shown in Fig. 1(a), we consider a suspension in a 2D box [17, 23, 27–30] $L \times L$ with periodic boundary conditions, consisting of N bacterial cell and a passive spherical tracer. Each cell is represented by a spherocylinder [17], with a diameter d , a length $2d$ and an orientation \mathbf{e}_i denoting the swimming direction (inset). Fig. 1(b) shows the tracers used in our simulations. The coated portion with a constant surface concentration c_0 is colored orange, while non-coated portion is colored blue. Both the hard bod-

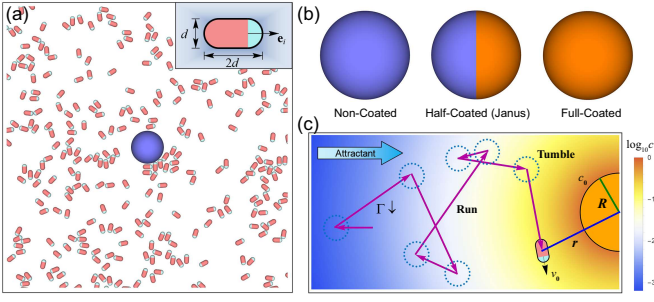


FIG. 1. (a) The snapshot of simulation system, where the bacterial cell is represented by spherocylinder as depicted in inset. (b) Three types of tracer used in our simulations. The coated and non-coated portions are colored orange and blue respectively. (c) Schematic diagram of the motion of run-and-tumble bacteria in a chemoattractant-concentration field c generated by the coated portion of tracer.

ies of bacterial cell and tracer are modeled by the sum of identical force centers with short-range repulsive potentials [17]. Details of the mechanical interactions are given in Supplemental Material [31] and depicted in Fig. S1. In addition, to mimic the run-and-tumble motion of bacteria, a constant drift velocity v_0 along e_i is added on the cell in running state to create a straight swim, while a random torque is exerted during the tumbling state to randomize the direction of next run. At each time step, the running cell has a probability $\Gamma\delta t$ to switch in a tumbling state, and a probability $\Xi\delta t$ to switch back, where δt is the time interval. Realistic physical value suitable for motile *E. coli* cells [23, 26], can be obtained as $d = 1.5\mu\text{m}$, $v_0 = 30\mu\text{m/s}$, $\Xi = 10\text{s}^{-1}$, $\Gamma = 1\text{s}^{-1}$ (without chemotactic response). The radius of tracer R is $5.07\mu\text{m}$ [30], in line with those previous experimental works [20, 21]. Box size L is set as $160\mu\text{m}$. Runge-Kutta method [32] is used for numerical integration with $\delta t = 10^{-4}\text{s}$. To examine the validity of this model, simulations of bacterial bath with non-coated tracer are performed. The results (Fig. S2) are highly consistent with pervious experiments [20, 21], demonstrating that bacterial motion can indeed be reproduced by this model.

Moreover, the chemotactic response of bacteria is realized by changing Γ based on the concentration of chemoattractant. As shown in Fig. 1(c), Γ will be lowered to extend runs when bacterium moves up the gradient of attractants [26]. This process is quantitatively simulated by MWC model [11, 12] and described in Supplemental Material [31] in detail. Next, to model the chemoattractant-concentration field generated by the coated portion of tracer, we assume that chemical spreads in the bath by classical diffusion, with diffusion constant D . Chemical also decays with a rate k in consequence of the enzymatic activity of bacteria. Therefore, the concentration field c obeys the reaction diffusion equation

[33–35]

$$\partial_t c(\mathbf{r}, t) = D\nabla^2 c - kc. \quad (1)$$

We use $D = 500\mu\text{m}^2/\text{s}$ based on the diffusivity of MeAsp [36], a widely used chemoattractant in experiments [11, 12, 36], and $k = 10\text{s}^{-1}$ [35]. The analytic solution of Eq. (1) can thereby be given, which rapidly reaches the steady state within 0.05s (Fig. S3). However, the displacement of tracer during the same time (about $0.1 - 0.3\mu\text{m}$ [31]) is much less than the tracer size. Thus, it is reasonable to assume that concentration field c is instantaneously stationary, i.e., $\partial_t c \equiv 0$, thereby making the field analytically solvable. The validity of model for chemotaxis is also proved by the reproduction of chemotactic aggregation [4] in such fields (Figs. S4 and S5, Movie I).

Based on this model, we firstly focus attention on the diffusion of full-coated tracer in bacterial suspension, where the chemotactic signal is homogenous. The concentration field for full-coated tracer is $c(r) = c_0 R e^{-\sqrt{k/D}(r-R)}/r$ [31], where r is the center-to-center distance between cell and tracer. We specialize to the case of $N = 784$ bacteria with number density $\phi = N/L^2 = 0.03/\mu\text{m}^2$, and systematically change the coating concentration c_0 . Average over 20 independent runs are performed. Fig. 2(a) shows the mean square displacement (MSD) $\langle \Delta x^2(t) \rangle = \langle |\mathbf{x}(t) - \mathbf{x}(0)|^2 \rangle$ for a wide range of c_0 , where $\mathbf{x}(t)$ is the position vector of tracer and $\langle \dots \rangle$ denotes the ensemble average. The tracer motion is short-time superdiffusive, i.e., $\langle \Delta x^2(t) \rangle \sim t^\gamma$ with diffusion exponent $\gamma > 1$, and becomes Fickian ($\gamma = 1$) at long time scales. The effective diffusion coefficient $D_{\text{eff}} = \lim_{t \rightarrow \infty} \langle \Delta x^2(t) \rangle / 4t$ is gradually raised when c_0 increases (inset), due to the enhanced perturbations exerted by bacteria in response to stronger chemotactic stimuli.

Moreover, to deepen understanding the statistics of tracer fluctuations, we calculate the 2D non-Gaussian parameter $\alpha_2(t) = \langle \Delta x^4(t) \rangle / 2 \langle \Delta x^2(t) \rangle^2 - 1$ [37] to characterize the heterogeneity of diffusion dynamics [Fig. 2(b)]. The dramatic departure of $\alpha_2(t)$ from 0 at short times shows the emergence of non-Gaussian statistics and a violation of central limit theorem (CLT). A perspective of such violation is that the environmental noise is strongly correlated during the characteristic time interval of athermal collisions [38], thereby making the sum of noises unable to converge in a Gaussian form as CLT describes at that time scale. Thus, to rationalize this perspective in our system, we use the Langevin formalism to describe the motion of tracer:

$$\dot{\mathbf{x}}(t) = \xi_B(t) + \xi_T(t), \quad (2)$$

where *bacterial noise* ξ_B denotes the perturbations exerted by bacteria and thermal noise ξ_T describes the collisions with solvent molecules. Here ξ_B satisfies $\langle \xi_B \rangle = 0$

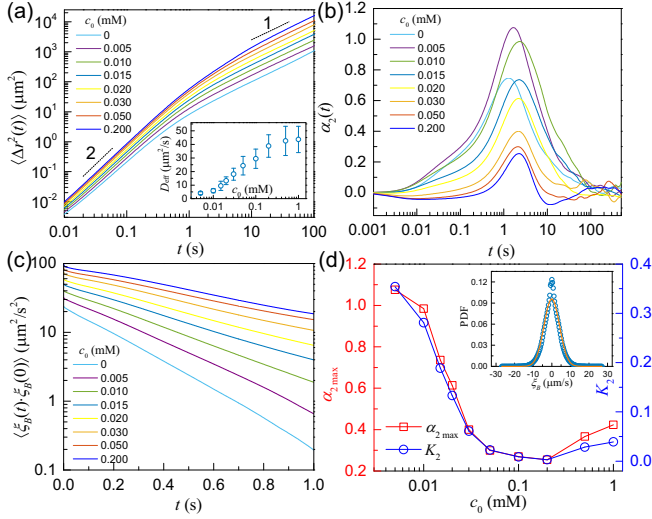


FIG. 2. Diffusion dynamics of full-coated tracer. (a) Mean square displacements for a wide range of c_0 . Inset: The plot of effective diffusion coefficient D_{eff} versus c_0 . (b) Non-Gaussian parameter $\alpha_2(t)$. (c) Autocorrelation functions of bacterial noise ξ_B . (d) The plots of $\alpha_{2\text{max}}$ and K_2 versus c_0 . Inset: Distribution of ξ_B when $c_0 = 0.005\text{mM}$ (circle). The solid line is the gaussian distribution with same variance.

due to the symmetrical signal, while ξ_T is a Gaussian white noise with zero mean and $\langle \xi_T(t) \cdot \xi_T(t') \rangle = 2D_t\delta(t - t')$. D_t is the diffusion coefficient of tracer in solvent. In particular, ξ_B can hardly be measured using experimental techniques, but can be easily obtained in simulations. Therefore, unlike previous experimental works [20, 25] where the correlation form can only be assumed, the correlation of bacterial noise in our system can directly be identified. For this purpose, corresponding autocorrelation functions $\langle \xi_B(t) \cdot \xi_B(0) \rangle$ are calculated, and are found to follow an exponential decay, as shown in Fig. 2(c). Hence, such correlation can be expressed as $\langle \xi_B(t) \cdot \xi_B(0) \rangle = \frac{\epsilon}{\tau}e^{-t/\tau}$, where ϵ and τ are the noise intensity and characteristic correlation time respectively, and both increase monotonically with c_0 (Fig. S6). The theoretical MSD can thereby be given:

$$\langle \Delta x^2(t) \rangle = 2\epsilon(t + \tau e^{-t/\tau} - \tau) + 4D_t t. \quad (3)$$

That is, the tracer diffusion is ballistic-like [$\langle \Delta x^2(t) \rangle = \frac{\epsilon}{\tau}t^2 + 4D_t t$] for $t \ll \tau$, and Fickian [$\langle \Delta x^2(t) \rangle \simeq 2(\epsilon + 2D_t)t$] for $t \gg \tau$, which is consistent with the results shown in Fig. 2(a). Therefore, it is confirmed that the change of diffusion pattern arises from the correlation of bacterial noise.

However, such correlation form cannot directly lead to a non-Gaussian statistics. One famous instance is the Ornstein-Uhlenbeck (OU) process $\dot{z}(t) = \xi_{OU}(t)$, where noise ξ_{OU} is also exponentially correlated [$\langle \xi_{OU}(t) \cdot \xi_{OU}(0) \rangle = \frac{\epsilon}{\tau}e^{-t/\tau}$] but Gaussian distributed [39]. By solving the corresponding master equation [40], the probability distribution $p(z, t)$ can be explicitly given with

initial condition $p(z, 0) = \delta(z)$, written in a Gaussian form as $p(z, t) = \exp(-\frac{z^2}{2\sigma(t)})/\sqrt{2\pi\sigma(t)}$, where $\sigma(t) = \epsilon(t + \tau e^{-t/\tau} - \tau)$. Hence, OU process is governed by CLT, quite different from the tracer statistic where the displacement distribution is strongly non-Gaussian (Fig. S7). Therefore, unlike ξ_{OU} , ξ_B must be a non-Gaussian (athermal) noise, as predicted by the aforementioned perspective. We further confirm the non-Gaussianity of ξ_B by measuring corresponding probability distribution [inset of Fig. 2(d)]. To quantitatively reveal the relation between non-Gaussian statistics and bacterial noise, the non-Gaussian parameter of ξ_B , defined as $K_2 = \langle \xi_B^4 \rangle / 3\langle \xi_B^2 \rangle^2 - 1$, is also calculated. As shown in Fig. 2(d), K_2 and the maximum of $\alpha_2(t)$, $\alpha_{2\text{max}}$, which characterizes the non-Gaussian level of tracer statistics, show same dependence on c_0 . Such strong correlation between K_2 and $\alpha_{2\text{max}}$ corroborates that the non-Gaussian statistics of tracer indeed originates from the athermal bacterial noise.

In striking contrast to full-coated tracer where the concentration field is spherically symmetrical, breaking the symmetry of chemotactic signal can directly lead to a biased bacterial noise ($\langle \xi_B \rangle \neq 0$), thereby complicating the tracer fluctuation by persistent drifts exerted by bacteria. Thus, to quantitatively capture the potential peculiarities of tracer statistics brought by asymmetrical effects, we investigate the diffusion dynamics of a half-coated (Janus) tracer immersed in bacterial bath. By solving Eq. (1), corresponding concentration field can be expressed as [31]

$$c(r, \theta) = c_0 \sum_{n=0}^{\infty} a_n k_n(\lambda r) P_n(\cos \theta), \quad (4)$$

where $P_n(t)$ and $k_n(t)$ ($n = 0, 1, 2, 3, \dots$) are the Legendre polynomial and modified spherical Bessel function of the second kind, respectively. The definition of θ is delineated in the top inset of Fig. 3(a). a_n is determined by boundary condition, given by $a_n = \frac{2n+1}{2k_n(\lambda R)} \int_0^1 P_n(t) dt$ where $\lambda = \sqrt{k/D}$.

We focus on the system where $\phi = 0.03/\mu\text{m}^2$ as well, and systematically change the coating concentration c_0 . Unlike the motion of full-coated tracer which is always long-time Brownian, Janus tracer demonstrates two distinct transport patterns for different c_0 . Representative trajectories of such two patterns are shown in Fig. 3(a) for $c_0 = 0.04$ (main view) and 1.0mM (bottom inset) respectively. For low coating concentration (e.g., $c_0 = 0.04\text{mM}$), the trajectory appears random to the eye. However, differing from conventional Brownian transport where each step is statistically identical, the tracer alternatively performs persistent walks and local jiggling, which are schematically indicated by arrows and dashed circles respectively. To reveal the inner nature of this unusual randomness, a wavelet-based method [41] is employed to rapidly separate the persistent “active” runs

from random “passive” jiggling. The active portions of tracked positions (partially shown as grey dots) detected by wavelet analysis are highlighted by grey circles in Fig. 3(a). To uncover the underlying differences between these active and passive steps, we denote the length of active or passive segment as “step size”, l , and measure the corresponding probability distributions $p(l)$ based on over 100 independent trajectories. As shown in Fig. 3(b), the size of passive step is exponentially distributed (highlighted in inset), indicating that statistics of local jiggling obeys the descriptions of classic Brownian random walks [42]. More intriguingly, for active steps, a power-law tail with slope $\mu = -2$ can be identified. Such power-law tail suggests that active steps follow the landscape of Lévy flights, where the distribution of step size is heavy-tailed with slope μ satisfying $-3 < \mu < -1$ [43]. Therefore, the transport of Janus tracer at low coating concentration is identified to be a composite random walk (CRW) combining power-law-tail distributed Lévy flights with Brownian jiggling. However, such CRW doesn’t hold for high coating concentration (e.g., $c_0 = 1.0\text{mM}$), where the tracer motion maintains directional persistence as delineated in the bottom inset of Fig. 3(a). Such reinforcing directionality can be quantitatively characterized by the distribution of *turning angles*, which are determined by an error-radius analysis (Fig. S8) [44]. As shown in Fig. 3(c), the uniformity of turning angles for $c_0 = 0.04\text{mM}$ (top) implies that no direction is preferred for turns in CRW, while the biased distribution for $c_0 = 1.0\text{mM}$ (bottom) shows that the corresponding transport is statistically directional. Hence, a “phase” transition for Janus tracer can be identified, from a composite random walk to an enhanced directional transport (EDT) when increasing the coating concentration.

In particular, such transition can be directly captured by the long-time diffusion exponent γ_L , which is deter-

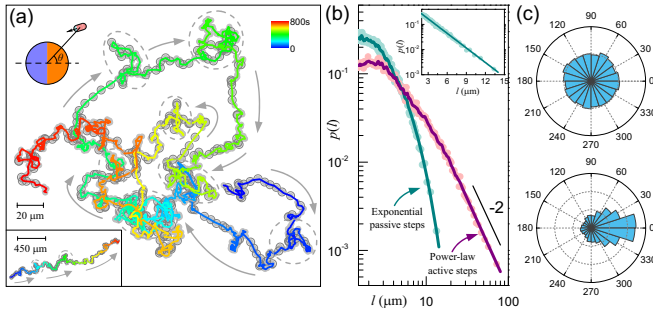


FIG. 3. Transport of Janus tracer. (a) Representative trajectories tracked for 800s when $c_0 = 0.04$ (main view) and 0.1mM (bottom inset) respectively. The top inset denotes the definition of θ . (b) The probability distribution of step size plotted in log-log scale, showing exponential statistics for passive steps (replotted in inset) and power-law tail with slope -2 for active steps, respectively. (c) Distributions of turning angles for $c_0 = 0.04$ (top) and 0.1mM (bottom).

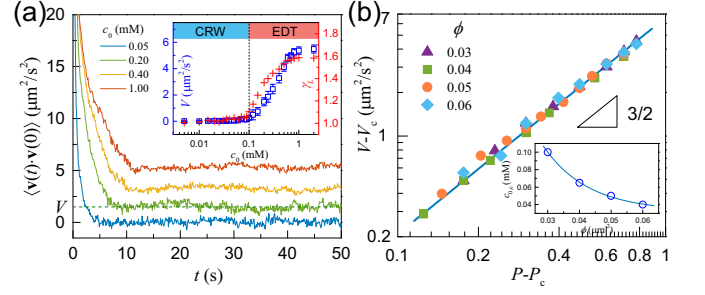


FIG. 4. (a) Time evolution of VACFs for various c_0 . The green dashed line shows the value of V when $c_0 = 0.20\text{mM}$. Inset: the plot of V and γ_L versus c_0 . The dashed line denotes the critical point. (b) The log-log plot of $V - V_c$ versus $P - P_c$ for various bacterial densities ϕ . Inset: The critical points for different ϕ .

mined by $\langle \Delta r^2(t) \rangle \sim t^{\gamma_L}$ for long time scales. We use the MSD data between 10s and 100s to measure γ_L , and show the dependence of γ_L on c_0 in the inset of Fig. 4(a) as red crosses. The long-time transport of Janus tracer is found to be Fickian for CRW and superdiffusive for EDT, where the critical point of transition c_0^c can also be identified at $c_0 = 0.1\text{mM}$. However, the strict demarcation for “long time scales” is unclear, thereby making the measurement of γ_L influenced by the selection of time scales. Hence, a more precise approach to explore the origin of such transition is in great demand. Inspired by the relationship between MSD $\langle \Delta r^2(t) \rangle$ and velocity autocorrelation function (VACF) $\langle \mathbf{v}(t) \cdot \mathbf{v}(0) \rangle$, i.e., $\langle \Delta r^2(t) \rangle = \int_0^t ds(t-s) \langle \mathbf{v}(s) \cdot \mathbf{v}(0) \rangle$, we calculate the VACFs of tracer for various c_0 and show them in Fig. 4(a). Over sufficiently long times, VACF decays to zero for $c_0 < c_0^c$, and demonstrates a non-zero steady-state value (denoted as V) for $c_0 > c_0^c$. As expected, V and γ_L show the same dependence on c_0 [inset of Fig. 4(a), blue squares], corroborating that such approach can indeed capture the inner change of statistics when undergoing the phase transition. Since the tracer velocity mainly comes from the bacterial noise, the change of VACF definitely clarifies the mechanism of this CRW-to-EDT transition. That is, for CRW where the chemotactic signal is weak, the symmetry-breaking-induced drift exerted by bacteria is intermittent and can be dissipated, thereby making the transport short-time persistent for partial (active) steps and long-time Fickian. However, for EDT where the symmetry of stimuli is strongly broken, such drift is continuous, which directly leads to a superdiffusive movement that maintains directional persistence.

What is more striking is that VACF offers a quantitative way to identify the transition pattern. Note that the dependence of V upon c_0 (or $\log_{10} c_0$) is continuous-like, indicating such transition may be second-order. A central feature of second-order phase transition is that, physical quantities show power-law dependence with charac-

teristic critical exponents near critical point [45]. Hence, to probe this idea in our system, we look for an analogous critical behavior near c_0^c , expressed as

$$V - V_c \propto (P - P_c)^\beta, \quad (5)$$

where $P = \log_{10} c_0$ and β is the critical exponent. V_c and P_c are corresponding values for c_0^c . As shown in Fig. 4(b), $V - V_c$ versus $P - P_c$ demonstrates a power-law relation with critical exponent $\beta = 1.5$. Moreover, since critical exponent is usually system-independent [46], we systematically change the bacterial density ϕ to examine the universality of such behavior. As expected, despite that the critical point decreases with ϕ due to the increasing persistent drifts [inset of Fig. 4(b)], such power-law relation can still be identified, with β remaining 1.5 regardless of ϕ . Therefore, the CRW-to-EDT transition indeed conforms to the scenario of second-order phase transition.

In summary, we have presented what is to our knowledge the first theoretical investigation of tracer statistics in bacterial suspensions coupled with chemotactic effects, by developing a molecular dynamics model of bacterial chemotaxis. We demonstrate that the non-Gaussian statistics of full-coated tracer originates from bacterial noise, which is athermal and exponentially correlated. Moreover, upon increasing the coating concentration, a phase transition is discovered for half-coated tracer, from a composite random walk combining power-law-tail distributed Lévy flights with Brownian jiggling, to an enhanced directional transport. Such transition is identified to be second-order, with a critical exponent 1.5 independent of bacterial density. Our findings provide a significant advance in revealing the fundamental nonequilibrium physics of active matter under external stimuli, and suggest a novel approach for efficient cargo delivery utilizing stimulus-response technique and asymmetrical design.

We are thankful for helpful discussions with Ye Yang and Tianqi Cui. We acknowledge financial support from National Natural Science Foundation of China (Grant Nos. 21422403, 51273105, 51633003, 21174080). L.-T. Y. acknowledges financial support from Ministry of Science and Technology of China (Grant No. 2016YFA0202500).

* ltyan@mail.tsinghua.edu.cn

- [1] H. G. Hiscock, S. Worster, D. R. Kattnig, C. Steers, Y. Jin, D. E. Manolopoulos, H. Mouritsen, and P. J. Hore, *Proc. Natl. Acad. Sci. USA* **113**, 4634 (2016).
- [2] A. M. Edwards, R. A. Phillips, N. W. Watkins, M. P. Freeman, E. J. Murphy, V. Afanasyev, S. V. Buldyrev, M. G. E. da Luz, E. P. Raposo, H. E. Stanley, and G. M. Viswanathan, *Nature* **449**, 1044 (2007).
- [3] J. Adler, *Science* **153**, 708 (1966).
- [4] N. Mittal, E. O. Budrene, M. P. Brenner, and A. van Oudenaarden, *Proc. Natl. Acad. Sci. USA* **100**, 13259 (2003).
- [5] C. Carmona-Fontaine, H. K. Matthews, S. Kuriyama, M. Moreno, G. A. Dunn, M. Parsons, C. D. Stern, and R. Mayor, *Nature* **456**, 957 (2008).
- [6] H. C. Berg, *Random Walks in Biology* (Princeton University Press, 1993).
- [7] J. Alder and W.-W. Tso, *Science* **184**, 1292 (1974).
- [8] D. A. Brown and H. C. Berg, *Proc. Natl. Acad. Sci. USA* **71**, 1388 (1974).
- [9] J. E. Segall, S. M. Block, and H. C. Berg, *Proc. Natl. Acad. Sci. USA* **83**, 8987 (1986).
- [10] V. Sourjik and H. C. Berg, *Proc. Natl. Acad. Sci. USA* **99**, 123 (2002).
- [11] R. G. Endres and N. S. Wingreen, *Proc. Natl. Acad. Sci. USA* **103**, 13040 (2006).
- [12] Y. V. Kalinin, L. Jiang, Y. Tu, and M. Wu, *Biophys. J.* **96**, 2439 (2009).
- [13] A. Sahari, M. A. Traore, B. E. Scharf, and B. Behkam, *Biomed. Microdevices* **16**, 717 (2014).
- [14] G. H. Wadhams and J. P. Armitage, *Nature Rev. Mol. Cell Bio.* **5**, 1024 (2004).
- [15] A. Dhariwal, G. S. Sukhatme, and A. A. G. Requicha, eds., *Proceedings of the 2004 IEEE International Conference on Robotics & Automation* (IEEE, New Orleans, LA, 2004).
- [16] N. Koumakis, A. Lepore, C. Maggi, and R. D. Leonardo, *Nature Commun.* **4**, 2588 (2013).
- [17] L. Angelani, R. D. Leonardo, and G. Ruocco, *Phys. Rev. Lett.* **102**, 048104 (2009).
- [18] R. D. Leonardo, L. Angelani, D. DellArciprete, G. Ruocco, V. Iebba, S. Schippa, M. P. Conte, F. Mecarini, F. D. Angelis, and E. D. Fabrizio, *Proc. Natl. Acad. Sci. USA* **107**, 9541 (2010).
- [19] D. T. N. Chen, A. W. C. Lau, L. A. Hough, M. F. Islam, M. Goulian, T. C. Lubensky, and A. G. Yodh, *Phys. Rev. Lett.* **99**, 148302 (2007).
- [20] X.-L. Wu and A. Libchaber, *Phys. Rev. Lett.* **84**, 3017 (2000).
- [21] K. C. Leptos, J. S. Guasto, J. P. Gollub, A. I. Pesci, and R. E. Goldstein, *Phys. Rev. Lett.* **103**, 198103 (2009).
- [22] L. G. Wilson, V. A. Martinez, J. Schwarz-Linek, J. Tailleur, G. Bryant, P. N. Pusey, and W. C. K. Poon, *Phys. Rev. Lett.* **106**, 018101 (2011).
- [23] L. Angelani, C. Maggi, M. L. Bernardini, A. Rizzo, and R. D. Leonardo, *Phys. Rev. Lett.* **107**, 138302 (2011).
- [24] Y. Peng, L. Lai, Y.-S. Tai, K. Zhang, X. Xu, and X. Cheng, *Phys. Rev. Lett.* **116**, 068303 (2016).
- [25] N. Darnton, L. Turner, K. Breuer, and H. C. Berg, *Biophys. J.* **86**, 1863 (2004).
- [26] H. C. Berg, *E. Coli in Motion* (Springer-Verlag, New York, 2004).
- [27] J. Bialké, T. Speck, and H. Löwen, *Phys. Rev. Lett.* **108**, 168301 (2012).
- [28] G. S. Redner, M. F. Hagan, and A. Baskaran, *Phys. Rev. Lett.* **110**, 055701 (2013).
- [29] R. Ni, M. A. C. Stuart, and P. G. Bolhuis, *Phys. Rev. Lett.* **114**, 018302 (2015).
- [30] M. Rein, N. Hei, F. Schmid, and T. Speck, *Phys. Rev. Lett.* **116**, 058102 (2016).
- [31] See Supplemental Material for additional methods, movies, and figures.
- [32] W. H. Press, B. P. Flannery, S. A. Teukolsky, and W. T. Vetterling, *Numerical Recipes: The Art of Science*

- tific Computing*, 2nd ed. (Cambridge University Press).
- [33] A. Czirók, E. Ben-Jacob, I. Cohen, and T. Vicsek, *Phys. Rev. E* **54**, 1791 (1996).
 - [34] R. Grima, *Phys. Rev. Lett.* **95**, 128103 (2005).
 - [35] J. Taktikos, V. Zaburdaev, and H. Stark, *Phys. Rev. E* **84**, 041924 (2011).
 - [36] M. D. Lazova, T. Ahmed, D. Bellomo, R. Stocker, and T. S. Shimizu, *Proc. Natl. Acad. Sci. USA* **108**, 13870 (2011).
 - [37] J. Kim, C. Kim, and B. J. Sung, *Phys. Rev. Lett.* **110**, 047801 (2013).
 - [38] K. Kanazawa, T. G. Sano, T. Sagawa, and H. Hayakawa, *Phys. Rev. Lett.* **114**, 090601 (2015).
 - [39] A. H. Romero and J. M. Sancho, *J. Comput. Phys.* **156**, 1 (1999).
 - [40] P. Hänggi and H. Thomas, *Z. Phys. B* **26**, 85 (1977).
 - [41] K. Chen, B. Wang, J. Guan, and S. Granick, *ACS Nano* **7**, 8634 (2013).
 - [42] E. A. Codling, M. J. Plank, and S. Benhamou, *J. R. Soc. Interface* **5**, 813 (2008).
 - [43] M. J. Plank, M. Auger-Méthé, and E. A. Codling, in *Dispersal, Individual Movement and Spatial Ecology: A Mathematical Perspective*, edited by M. A. Lewis, P. K. Maini, and S. V. Petrovskii (Springer, Heidelberg, 2013) Chap. 2, pp. 33–52, 1st ed.
 - [44] K. Chen, B. Wang, and S. Granick, *Nature Mater.* **14**, 589 (2015).
 - [45] A. Doron, I. Tamir, S. Mitra, G. Zeltzer, M. Ovadia, and D. Shahar, *Phys. Rev. Lett.* **116**, 057001 (2016).
 - [46] J. M. Yeomans, *Statistical Mechanics of Phase Transitions* (Clarendon Press, 1992).